

BCS-BEC crossover at finite temperature in spin-orbit coupled Fermi gases

Lianyi He,^{1,*} Xu-Guang Huang,^{1,2,†} Hui Hu,³ and Xia-Ji Liu³

¹Frankfurt Institute for Advanced Studies and Institute for Theoretical Physics,
J. W. Goethe University, 60438 Frankfurt am Main, Germany

²Physics Department and Center for Exploration of Energy and Matter,
Indiana University, 2401 N Milo B. Sampson Lane, Bloomington, IN 47408, USA

³ARC Centre of Excellence for Quantum-Atom Optics, Centre for Atom Optics and Ultrafast Spectroscopy,
Swinburne University of Technology, Melbourne 3122, Australia

(Dated: July 4, 2018)

By adopting a T -matrix-based method within the G_0G approximation for the pair susceptibility, we study the effects of the pairing fluctuation on the three-dimensional spin-orbit-coupled Fermi gases at finite temperature. The critical temperatures of the superfluid to normal phase transition are determined for three different types of spin-orbit coupling (SOC): (1) the extreme oblate (EO) or Rashba SOC, (2) the extreme prolate or equal Rashba-Dresselhaus SOC, and (3) the spherical (S) SOC. For EO- and S-type SOC, the SOC dependence of the critical temperature signals a crossover from BCS to BEC state; at strong SOC limit, the critical temperature recovers those of ideal BEC of rashbons. The pairing fluctuation induces a pseudogap in the fermionic excitation spectrum in both superfluid and normal phases. We find that, for EO- and S-type SOC, even at weak coupling, sufficiently strong SOC can induce sizable pseudogap. Our research suggests that the spin-orbit-coupled Fermi gases may open new means to the study of the pseudogap formation in fermionic systems.

PACS numbers: 03.75.Ss, 05.30.Fk, 67.85.Lm, 74.20.Fg

I. INTRODUCTION

The experimental realization of ultracold Fermi gases with tunable interatomic interaction has opened new era for the study of some longstanding theoretical proposals in many-fermion systems. One particular example is the smooth crossover from a Bardeen-Cooper-Schrieffer (BCS) superfluid ground state with largely overlapping Cooper pairs to a Bose-Einstein condensate (BEC) of tightly bound bosonic molecules – a phenomenon suggested many years ago [1–4]. For a dilute Fermi gas in three dimensions (3D) with a short-range interatomic interaction where the effective range r_0 of the interaction is much smaller than the interatomic distance, such a BCS-BEC crossover can be characterized by the dimensionless gas parameter, $1/(k_F a)$, where k_F is the Fermi momentum and a is the s -wave scattering length of the short-range interaction. The BCS-BEC crossover occurs when $1/(k_F a)$ is tuned from negative to positive values (the turning point is called unitarity).

This BCS-BEC crossover has been successfully demonstrated in ultracold Fermi gases where the s -wave scattering length is tuned by means of the Feshbach resonance [5–7]. This has been regarded as one of the key successes in the cold-atom researches and has attracted broad interests due to its special properties. For example, near unitarity, the system is a high- T_c superfluid: the superfluid to normal transition temperature T_c is much higher than that of an ordinary BCS superfluid. The normal state near unitarity is strongly affected by many-body effects, e.g., the pair fluctuations which we will thoroughly study, leading to deviations from a Fermi liquid

behavior and pseudogap opening, as in (underdoped) cuprate superconductors. Curiously, it is always interesting to look for other mechanisms of realizing the BCS-BEC crossover. Recent experimental breakthrough in generating synthetic non-Abelian gauge field in bosonic gas of ^{87}Rb atoms has opened the opportunity to study the spin-orbit-coupling (SOC) effects in cold atomic gases [8]. In this experiment, two counter propagating Raman laser beams and a transverse Zeeman field are applied to ^{87}Rb atoms, and three hyperfine levels of ^{87}Rb are coupled by the Raman lasers. By tuning the Zeeman field energy and the Raman laser frequency, two of the three hyperfine levels can become degenerate (which can be interpreted as two spins) and the low energy physics can be described by a model Hamiltonian of a spinor Bose gas coupled to an external spin $SU(2)$ non-Abelian gauge field which, in their special setup, turns out to induce a SOC. For the fermionic case, some of the recent theoretical results suggested that tuning the SOC may provide an alternative way to realize the BCS-BEC crossover [9–18]. The experimental exploration of the spin-orbit coupled Fermi gases has also achieved remarkable progresses and the Raman scheme designed for generating SOC in ^{87}Rb atoms has been successfully applied to Fermi gases: the spin-orbit coupled ^{40}K and ^6Li atoms have been realized at Shanxi University [19] and at Massachusetts Institute of Technology (MIT) [20], respectively.

The SOC of fermions can be induced by a synthetic uniform $SU(2)$ gauge field, $A_i^\mu = \lambda_i \delta_i^\mu$, where λ_i will play the roles of the SOC strengths. With this gauge field, the single-particle Hamiltonian reads $\mathcal{H} = \mathbf{k}^2/(2m) - \boldsymbol{\sigma} \cdot \mathbf{s}(\mathbf{k})$ where $\mathbf{s}(\mathbf{k}) = (\lambda_x k_x, \lambda_y k_y, \lambda_z k_z)$. In a very interesting paper [21], Vyasankere and Shenoy studied the two-body problem of this Hamiltonian. They paid particular attention to three special types of gauge field configurations: (1) $\lambda_x = \lambda_y = 0$ and $\lambda_z = \lambda$ [called extreme prolate (EP)], (2) $\lambda_x = \lambda_y = \lambda$ and $\lambda_z = 0$ [called extreme oblate (EO)], and (3) $\lambda_x = \lambda_y = \lambda_z$

*Electronic address: lianyi@fias.uni-frankfurt.de

†Electronic address: xuhuang@indiana.edu

[called spherical (S)]. The EO SOC is physically equivalent to the Rashba SOC which has been famous in condensed matter physics. The EP SOC is physically equivalent to an equal mixture of Rashba and Dresselhaus SOC. The most surprising finding of Vyasankere and Shenoy was that for EO and S SOC, even for $a < 0$ where the di-fermion bound state cannot form in the absence of SOC, the di-fermion bound state (referred to as rashbon) always exists and its binding energy is generally enhanced with increased SOC. Meanwhile, the bound state also possesses non-trivial effective mass which is generally larger than twice of the fermion mass m . For the two dimensional (2D) case, although a bound state exists for arbitrarily small attraction, it was shown in Ref. [16] that the EO or Rashba SOC can generally enhance the binding energy and the effective mass of the bound state.

The novel bound state that emerged in the two-body problem suggests that the EO or S SOC may trigger a new type of BCS-BEC crossover in the many-body problem of fermions. In fact, theoretical studies revealed that for EO or S SOC, even at small negative $k_F a$, a crossover from the BCS superfluid to the BEC of rashbons can be achieved by tuning the SOC λ to large enough value [9–18]. It was shown that for EO or S SOC the system enters the rashbon BEC regime at $\lambda \sim v_F$ where $v_F \equiv k_F/m$ is the Fermi velocity. Similar conclusions were also found for 2D Fermi gases with EO SOC [16].

So far, most of the theoretical studies of the BCS-BEC crossover in 3D SOC Fermi gases focused on the zero-temperature ground state based on mean-field theory (MFT). Although the MFT captures some qualitative features of the zero-temperature crossover, it loses the effects of the pairing fluctuation which becomes substantial when the system goes toward finite-temperature and/or the BEC regimes. In the absence of the SOC, previous theoretical studies [22–30] as well as quantum Monte Carlo simulation [31] have already revealed that, as a consequence of the pairing fluctuation, a “pseudogap” emerges in the fermionic excitation spectrum. This pseudogap is negligibly small at BCS limit but increases as $1/(k_F a)$ is increased and becomes significantly important on the BEC side. Particularly, the pseudogap survives above the superfluid critical temperature T_c and leads to an exotic normal state that is different from the Fermi-liquid normal state associated with the MFT. Recently, the experimental observation of pairing pseudogap in both 2D Fermi gases [32] and 3D Fermi gases [33] are reported. Similar pseudogap phenomena may also appear in other strongly correlated systems, such as high- T_c superconductors [22, 34–36], low-density nuclear matter [37], and color superconducting quark matter [38].

In this paper, we study the spin-orbit-coupled Fermi gases at finite temperature. To include the pairing-fluctuation effects and investigate the possible pseudogap phenomena, we will adopt a T -matrix formalism based on a G_0G approximation for the pair susceptibility which was first introduced by the Chicago group [23–28, 34]. This formalism generalizes the early works of Kadanoff and Martin [39] and Patton [40], and can be considered as a natural extension of the BCS theory since they share the same ground state. Moreover, this formalism allows quasi-analytic calculations and gives a

simple physical interpretation of the pseudogap emergence. It clearly shows that the pseudogap is due to the incoherent pairing fluctuation. Within this formalism, we can also determine the superfluid critical temperature and study how the pairing fluctuation affects the thermodynamics. We note that this is the first systematic study of the 3D spin-orbit-coupled Fermi gases at finite temperature. For 2D spin-orbit-coupled Fermi gases, the possible BKT transition at finite temperature was already studied [16].

The article is organized as follows. In Sec. II, we present a detailed theoretical scheme of the T -matrix-based formalism at finite temperature. The numerical results are given in Sec. III. We summarize in Sec. IV. Throughout this article, we use natural units $\hbar = k_B = 1$.

II. T-MATRIX-BASED FORMALISM

We consider a homogenous Fermi gas interacting via a short-range attractive interaction in the spin-singlet channel. In the dilute limit $k_F r_0 \ll 1$ and $m\lambda r_0 \ll 1$, where r_0 is the effective interaction range¹, this system can be described by the following Hamiltonian,

$$H = \int d^3\mathbf{r} \psi^\dagger(\mathbf{r}) (\mathcal{H}_0 + \mathcal{H}_{so}) \psi(\mathbf{r}) + U \int d^3\mathbf{r} \psi_\uparrow^\dagger(\mathbf{r}) \psi_\downarrow^\dagger(\mathbf{r}) \psi_\downarrow(\mathbf{r}) \psi_\uparrow(\mathbf{r}), \quad (2.1)$$

where $\mathcal{H}_0 = -\nabla^2/(2m) - \mu$ is the free single-particle Hamiltonian with μ being the chemical potential, $\mathcal{H}_{so} = -i \sum_{i=1}^3 \lambda_i \sigma_i \partial_i$ is the SOC term, and $U < 0$ denotes the attractive s -wave interaction.

Introduce the four-dimensional Nambu-Gorkov spinor $\Psi = (\psi_\uparrow, \psi_\downarrow, \psi_\uparrow^\dagger, \psi_\downarrow^\dagger)^T$. The (imaginary-time) Green’s function of the Nambu-Gorkov spinor is given by

$$\mathcal{S}(\tau, \mathbf{r}) \equiv -\langle T_\tau \Psi(\tau, \mathbf{r}) \Psi^\dagger(0, \mathbf{0}) \rangle = \begin{bmatrix} \mathcal{G}(\tau, \mathbf{r}) & \mathcal{F}(\tau, \mathbf{r}) \\ \tilde{\mathcal{F}}(\tau, \mathbf{r}) & \tilde{\mathcal{G}}(\tau, \mathbf{r}) \end{bmatrix}, \quad (2.2)$$

where T_τ is the (imaginary-) time-ordering operator and $\tau \equiv it$. It is convenient to work in frequency-momentum space,

$$\mathcal{S}(K) = \begin{bmatrix} \mathcal{G}(K) & \mathcal{F}(K) \\ \tilde{\mathcal{F}}(K) & \tilde{\mathcal{G}}(K) \end{bmatrix}, \quad (2.3)$$

where $K = (k_0 \equiv i\omega_n, \mathbf{k})$ with $\omega_n = (2n + 1)\pi T$ (n integer) being the Matsubara frequency for fermion. The Green’s

¹ The interaction range r_0 is about 3.2 nm for ⁴⁰K [41] and 2.1 nm for ⁶Li [42]. Thus for these atoms when $k_F, m\lambda \gtrsim 0.1 \text{ nm}^{-1}$ the dilute condition may be violated. In Shanxi University experiment [19], $m\lambda = 0.008 \text{ nm}^{-1}$ and k_F varies from $0.9m\lambda$ to $1.8m\lambda$; in MIT experiment [20], $m\lambda = 0.003 \text{ nm}^{-1}$ and k_F varies about $m\lambda$. In both experiments, the dilute conditions are well satisfied.

functions have the following properties:

$$\tilde{\mathcal{G}}(i\omega_n, \mathbf{k}) = -[\mathcal{G}(-i\omega_n, -\mathbf{k})]^T, \quad (2.4)$$

$$\tilde{\mathcal{F}}(i\omega_n, \mathbf{k}) = +[\mathcal{F}(-i\omega_n, \mathbf{k})]^\dagger, \quad (2.5)$$

$$\mathcal{F}(i\omega_n, \mathbf{k}) = -[\mathcal{F}(-i\omega_n, -\mathbf{k})]^T, \quad (2.6)$$

$$\tilde{\mathcal{F}}(i\omega_n, \mathbf{k}) = -[\tilde{\mathcal{F}}(-i\omega_n, -\mathbf{k})]^T, \quad (2.7)$$

$$\mathcal{G}(i\omega_n, \mathbf{k}) = +[\mathcal{G}(-i\omega_n, \mathbf{k})]^\dagger, \quad (2.8)$$

$$\tilde{\mathcal{G}}(i\omega_n, \mathbf{k}) = +[\tilde{\mathcal{G}}(-i\omega_n, \mathbf{k})]^\dagger. \quad (2.9)$$

In the rest of this section, we will introduce the basic method of the T -matrix. Our strategy will closely follow Refs. [23–28, 34, 37]. The T -matrix we will adopt is defined as an infinite series of ladder-diagrams in the particle-particle channel by constructing the ladder by one free particle propagator and one full particle propagator. The T -matrix thus enters the particle self-energy in place of the bare interaction vertex. The equation that defines the T -matrix, the self-energy equation (or gap equation) as well as the number density equation form a closed set of equations, and should be solved consistently. One can view this approach as the simplest generalization of the BCS theory, which can also be cast formally into a T -matrix formalism. Let us start with the BCS theory.

A. BCS Theory

The BCS theory is based on the mean-field approximation to the anomalous self-energy. We start with the mean-field inverse fermion propagator,

$$\mathcal{S}_{\text{mf}}^{-1}(K) = \begin{bmatrix} \mathcal{G}_0^{-1}(K) & i\sigma_y \Delta_{\text{mf}} \\ -i\sigma_y \Delta_{\text{mf}} & -[\mathcal{G}_0^{-1}(-K)]^T \end{bmatrix}, \quad (2.10)$$

where the anomalous self-energy Δ_{mf} is chosen as a constant and can be used as an order parameter for superfluid phase transition. The inverse free fermion propagator reads,

$$\mathcal{G}_0^{-1}(K) = i\omega_n - \xi_{\mathbf{k}} - \xi_{\text{so}}(\mathbf{k}), \quad (2.11)$$

with $\xi_{\mathbf{k}} = \mathbf{k}^2/(2m) - \mu$ and $\xi_{\text{so}}(\mathbf{k}) = \sum_{i=1}^3 \lambda_i \sigma_i k_i$ (λ_i is real). By direct doing the matrix inversion, one obtains

$$\mathcal{S}_{\text{mf}}(K) = \begin{bmatrix} \mathcal{G}_{\text{mf}}(K) & \mathcal{F}_{\text{mf}}(K) \\ \tilde{\mathcal{F}}_{\text{mf}}(K) & \tilde{\mathcal{G}}_{\text{mf}}(K) \end{bmatrix}. \quad (2.12)$$

Its elements are

$$\mathcal{G}_{\text{mf}}(K) = \mathcal{A}_{11}(K) + \frac{\xi_{\text{so}}(\mathbf{k})}{\lambda|\mathbf{k}|} \mathcal{B}_{11}(K), \quad (2.13)$$

$$\tilde{\mathcal{G}}_{\text{mf}}(K) = \mathcal{A}_{22}(K) + \frac{\xi_{\text{so}}^*(\mathbf{k})}{\lambda|\mathbf{k}|} \mathcal{B}_{22}(K), \quad (2.14)$$

$$\mathcal{F}_{\text{mf}}(K) = -i\sigma_y \left[\mathcal{A}_{12}(K) + \frac{\xi_{\text{so}}^*(\mathbf{k})}{\lambda|\mathbf{k}|} \mathcal{B}_{12}(K) \right], \quad (2.15)$$

$$\tilde{\mathcal{F}}_{\text{mf}}(K) = i\sigma_y \left[\mathcal{A}_{21}(K) + \frac{\xi_{\text{so}}(\mathbf{k})}{\lambda|\mathbf{k}|} \mathcal{B}_{21}(K) \right], \quad (2.16)$$

where we introduced $\lambda|\mathbf{k}| \equiv \sqrt{\sum_{i=1}^3 \lambda_i^2 k_i^2}$ and

$$\begin{aligned} \mathcal{A}_{11}(K) &= \frac{1}{2} \left[\frac{i\omega_n + \xi_{\mathbf{k}}^+}{(i\omega_n)^2 - (E_{\mathbf{k}}^+)^2} + \frac{i\omega_n + \xi_{\mathbf{k}}^-}{(i\omega_n)^2 - (E_{\mathbf{k}}^-)^2} \right], \\ \mathcal{A}_{22}(K) &= \frac{1}{2} \left[\frac{i\omega_n - \xi_{\mathbf{k}}^+}{(i\omega_n)^2 - (E_{\mathbf{k}}^+)^2} + \frac{i\omega_n - \xi_{\mathbf{k}}^-}{(i\omega_n)^2 - (E_{\mathbf{k}}^-)^2} \right], \\ \mathcal{A}_{12}(K) &= \frac{1}{2} \left[\frac{\Delta_{\text{mf}}}{(i\omega_n)^2 - (E_{\mathbf{k}}^+)^2} + \frac{\Delta_{\text{mf}}}{(i\omega_n)^2 - (E_{\mathbf{k}}^-)^2} \right], \\ \mathcal{A}_{21}(K) &= \mathcal{A}_{12}(K) \end{aligned} \quad (2.17)$$

and

$$\begin{aligned} \mathcal{B}_{11}(K) &= \frac{1}{2} \left[\frac{i\omega_n + \xi_{\mathbf{k}}^+}{(i\omega_n)^2 - (E_{\mathbf{k}}^+)^2} - \frac{i\omega_n + \xi_{\mathbf{k}}^-}{(i\omega_n)^2 - (E_{\mathbf{k}}^-)^2} \right], \\ \mathcal{B}_{22}(K) &= -\frac{1}{2} \left[\frac{i\omega_n - \xi_{\mathbf{k}}^+}{(i\omega_n)^2 - (E_{\mathbf{k}}^+)^2} - \frac{i\omega_n - \xi_{\mathbf{k}}^-}{(i\omega_n)^2 - (E_{\mathbf{k}}^-)^2} \right], \\ \mathcal{B}_{12}(K) &= -\frac{1}{2} \left[\frac{\Delta_{\text{mf}}}{(i\omega_n)^2 - (E_{\mathbf{k}}^+)^2} - \frac{\Delta_{\text{mf}}}{(i\omega_n)^2 - (E_{\mathbf{k}}^-)^2} \right], \\ \mathcal{B}_{21}(K) &= -\mathcal{B}_{12}(K). \end{aligned} \quad (2.18)$$

Here $E_{\mathbf{k}}^\pm = \sqrt{(\xi_{\mathbf{k}}^\pm)^2 + \Delta_{\text{mf}}^2}$ with $\xi_{\mathbf{k}}^\pm = \xi_{\mathbf{k}} \pm \lambda|\mathbf{k}|$ is the fermion dispersion relation. One can verify that Eqs. (2.13)-(2.16) satisfy Eqs. (2.4)-(2.9).

Then from the standard Green's function method, the coupled gap and density equations are expressed as

$$\begin{aligned} \Delta_{\text{mf}} &= -\frac{U}{2\beta V} \text{Tr} \sum_K i\sigma_y \mathcal{F}_{\text{mf}}(K) \\ &= -\frac{U\Delta_{\text{mf}}}{2V} \sum_{\alpha=\pm} \sum_{\mathbf{k}} \frac{1 - 2n_F(E_{\mathbf{k}}^\alpha)}{2E_{\mathbf{k}}^\alpha}, \\ n &= \frac{1}{\beta V} \text{Tr} \sum_K e^{i\eta\omega_n} \mathcal{G}_{\text{mf}}(K) \\ &= \frac{1}{V} \sum_{\alpha=\pm} \sum_{\mathbf{k}} [(u_{\mathbf{k}}^\alpha)^2 n_F(E_{\mathbf{k}}^\alpha) + (v_{\mathbf{k}}^\alpha)^2 n_F(-E_{\mathbf{k}}^\alpha)], \end{aligned} \quad (2.19)$$

where $n_F(x) = 1/[\exp(\beta x) + 1]$ is the Fermi-Dirac function, $e^{i\eta\omega_n}$ with $\eta \rightarrow 0^+$ is a convergence factor for the Matsubara summation, and $(u_{\mathbf{k}}^\alpha)^2 = \frac{1}{2}(1 + \xi_{\mathbf{k}}^\alpha/E_{\mathbf{k}}^\alpha)$ and $(v_{\mathbf{k}}^\alpha)^2 = \frac{1}{2}(1 - \xi_{\mathbf{k}}^\alpha/E_{\mathbf{k}}^\alpha)$ are the Bogoliubov coefficients.

The difference between $\mathcal{G}_0^{-1}(K)$ and $\mathcal{G}_{\text{mf}}^{-1}(K)$ defines the mean-field self-energy,

$$\begin{aligned} \Sigma_{\text{mf}}(K) &= \mathcal{G}_0^{-1}(K) - \mathcal{G}_{\text{mf}}^{-1}(K) \\ &= -\Delta_{\text{mf}}^2 i\sigma_y \tilde{\mathcal{G}}_0(K) i\sigma_y. \end{aligned} \quad (2.21)$$

If we define a T matrix in the following form,

$$t_{\text{mf}}(Q) = -\Delta_{\text{mf}}^2 \delta(Q), \quad (2.22)$$

where $Q = (q_0 \equiv i\omega_\nu, \mathbf{q})$ with $\omega_\nu = 2\nu\pi T$ (ν integer) being the boson Matsubara frequency and $\delta(Q) = \beta\delta_{\nu,0}\delta^{(3)}(\mathbf{q})$, Eq. (2.21) can be rewritten in a manner of

$$\Sigma_{\text{mf}}(K) = \frac{1}{\beta V} \sum_Q t_{\text{mf}}(Q) i\sigma_y \tilde{\mathcal{G}}_0(K - Q) i\sigma_y. \quad (2.23)$$

This shows that in the BCS theory, the fermion-fermion pairs contribute to the fermion self-energy only through their condensate at zero momentum, and these *condensed* pairs are associated with a T -matrix or propagator (2.22).

Furthermore, if we define the mean-field pair susceptibility as

$$\chi_{\text{mf}}(Q) = \frac{1}{2\beta V} \text{Tr} \sum_K \left[\mathcal{G}_{\text{mf}}(K) i\sigma_y \tilde{\mathcal{G}}_0(K-Q) i\sigma_y \right], \quad (2.24)$$

we can rewrite the gap equation in the superfluid phase as

$$1 + U\chi_{\text{mf}}(0) = 0, \quad T \leq T_c. \quad (2.25)$$

This suggests that if one considers the *uncondensed* pair propagator or T matrix to be of the form

$$t_{\text{pair}} = \frac{U}{1 + U\chi_{\text{mf}}(Q)}, \quad Q \neq 0, \quad (2.26)$$

then the gap equation is given by $t_{\text{pair}}^{-1}(0) = 0$.

It is well known that the critical temperature T_c in the BCS theory is related to the appearance of a singularity in a T matrix in the form of Eq. (2.26) but with $\Delta_{\text{mf}} = 0$. This is the so-called Thouless criterion for T_c [43]. But the meaning of Eq. (2.25) is more general as stressed by Kadanoff and Martin [39]. It states that under an asymmetric choice of χ_{mf} , the gap equation is equivalent to the requirement that the T matrix associated with the uncondensed pairs remains singular at zero momentum and frequency for all temperatures below T_c .

Although the construction of the uncondensed pair propagator (2.26) in BCS scheme is quite natural, the uncondensed pair has no feedback to the fermion self-energy (2.23). In the BCS limit (both $|U|$ and λ are small), such a feedback may not be important, but if the system is strongly coupled (for large $|U|$ and/or for large λ for EO or S SOC), this feedback will be essential. The simplest way to include the feedback effects is to replace t_{mf} in Eq. (2.23) by $t_{\text{mf}} + t_{\text{pair}}$. But to make such an inclusion self-consistent, t_{pair} should be somewhat modified which we now discuss.

B. G_0G Formalism at $T \leq T_c$

The BCS theory involves the contribution to the self-energy from the condensed pairs only, but generally, in superfluid phase, the self-energy consists of two distinctive contributions, one from the superfluid condensate, and the other from thermal or quantum pair fluctuations. Correspondingly, it is natural to decompose the self-energy into two additive terms,

$$\begin{aligned} \Sigma(K) &= \frac{1}{\beta V} \sum_Q t(Q) i\sigma_y \tilde{\mathcal{G}}_0(K-Q) i\sigma_y \\ &= \Sigma_{\text{sf}}(K) + \Sigma_{\text{pg}}(K), \end{aligned} \quad (2.27)$$

with the T matrix accordingly given by

$$\begin{aligned} t(Q) &= t_{\text{sf}}(Q) + t_{\text{pg}}(Q), \\ t_{\text{sf}}(Q) &= -\Delta_{\text{sf}}^2 \delta(Q), \\ t_{\text{pg}}(Q) &= \frac{U}{1 + U\chi(Q)}, \quad Q \neq 0, \end{aligned} \quad (2.28)$$

where the subscript sf and pg indicate that these terms are responsible to the superfluid condensate and pseudogap in fermionic dispersion relation. See Fig. 1 for the Feynman diagrams for $t_{\text{pg}}(Q)$ and $\Sigma(K)$. Comparing with the BCS scheme, $t_{\text{mf}}(Q)$ in Eq. (2.23) is replaced by $t(Q)$, and $\Sigma(K)$ now contains the feedback of uncondensed pairs. Inspired by Eq. (2.24), we now choose the pair susceptibility $\chi(Q)$ to be the following asymmetric G_0G form,

$$\chi(Q) = \frac{1}{2\beta V} \sum_K \mathcal{G}(K) i\sigma_y \tilde{\mathcal{G}}_0(K-Q) i\sigma_y. \quad (2.29)$$

In spirit of Kadanoff and Martin, we now propose the superfluid instability condition or gap equation as [extension of Eq. (2.25)]

$$1 + U\chi(0) = 0, \quad T \leq T_c. \quad (2.30)$$

We stress here that this condition has quite clear physical meaning in BEC regime. The dispersion relation of the bound pair is given by $t_{\text{pg}}^{-1}(Q) = 0$, hence $t_{\text{pg}}^{-1}(0) \propto \mu_b$ with μ_b the effective chemical potential of the pairs. Then the BEC condition requires $\mu_b = 0$, and thus $t_{\text{pg}}^{-1}(Q) = 0$, for all $T \leq T_c$.

The gap equation (2.30) tells us that $t_{\text{pg}}(Q)$ is highly peaked around $Q = 0$, so we can approximate Σ_{pg} as

$$\Sigma_{\text{pg}}(K) \simeq -\Delta_{\text{pg}}^2 i\sigma_y \tilde{\mathcal{G}}_0(K) i\sigma_y, \quad T \leq T_c, \quad (2.31)$$

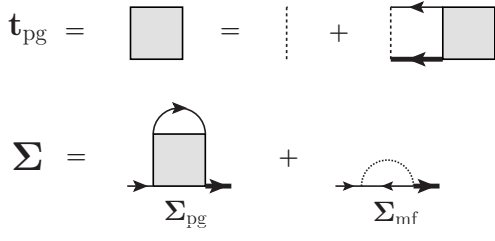
where we have defined the pseudogap parameter Δ_{pg} via

$$\Delta_{\text{pg}}^2 = -\frac{1}{\beta V} \sum_{Q \neq 0} t_{\text{pg}}(Q). \quad (2.32)$$

The total self-energy now is written in a BCS-type form

$$\Sigma(K) = -\Delta^2 i\sigma_y \tilde{\mathcal{G}}_0(K) i\sigma_y, \quad (2.33)$$

but with $\Delta^2 = \Delta_{\text{sf}}^2 + \Delta_{\text{pg}}^2$. It is clear that Δ_{pg} also contributes to the energy gap in fermionic excitation. Physically, the pseudogap Δ_{pg} below T_c can be interpreted as extra contribution to the excitation gap of fermion: an additional energy is needed to overcome the residual binding between fermions in a thermal excited pair to produce fermion-like quasi-particles. One should note that Δ_{pg} is associated with the thermal fluctuation of the pairs $\Delta_{\text{pg}}^2(T) \sim \langle \Delta^2(T) \rangle - \langle \Delta(T) \rangle^2$ [25, 34] hence it does not lead to superfluid (symmetry breaking). Besides, at $T = 0$, the G_0G formalism recovers the BCS theory, hence the G_0G formalism does not involve quantum fluctuation. We note here that at strong interacting regime the quantum fluctuations could have sizable contributions to certain quantities like the excitation gap. For example, at the unitarity and at $T = 0$, the G_0G approach gives $\Delta \approx 0.69\epsilon_{\text{F}}$ (see, for



with $q_0 = i\omega_\nu$ and

$$\mathcal{T}_{\mathbf{k}\mathbf{q}} = \sum_{i=1}^3 \frac{\lambda_i^2 k_i (q_i - k_i)}{\lambda^2 |\mathbf{k}| |\mathbf{q} - \mathbf{k}|}. \quad (2.37)$$

FIG. 1: Feynman diagrams for the T matrix of non-condensed pairs and the fermion self-energy in the G_0G formalism.

example, Sec. III C) while quantum Monte Carlo simulation gives $\Delta \approx 0.54\varepsilon_F$ [44]. So neglecting the quantum fluctuations in the G_0G formalism gives roughly a 30% inaccuracy at $T = 0$ for the superfluid gap near unitarity.

With the self-energy (2.33), it is easy to see that the gap equation and number equation remain the forms of Eqs. (2.19)-(2.20) except the replacement of $\Delta_{\text{mf}} \rightarrow \Delta$:

$$1 = -\frac{U}{2V} \sum_{\alpha=\pm} \sum_{\mathbf{k}} \frac{1 - 2n_F(E_{\mathbf{k}}^\alpha)}{2E_{\mathbf{k}}^\alpha}, \quad (2.34)$$

$$n = \frac{1}{\beta V} \text{Tr} \sum_K e^{i\eta\omega_n} \mathcal{G}(K)$$

$$= \frac{1}{V} \sum_{\alpha=\pm} \sum_{\mathbf{k}} [(u_{\mathbf{k}}^\alpha)^2 n_F(E_{\mathbf{k}}^\alpha) + (v_{\mathbf{k}}^\alpha)^2 n_F(-E_{\mathbf{k}}^\alpha)]. \quad (2.35)$$

The pair susceptibility (2.29) can be calculated as,

$$\chi(Q) = \frac{1}{4V} \sum_{\alpha,\gamma,s=\pm} \sum_{\mathbf{k}} \frac{1}{2} \left(1 + s \frac{\xi_{\mathbf{k}}^\alpha}{E_{\mathbf{k}}^\alpha}\right) (1 - \alpha\gamma\mathcal{T}_{\mathbf{k}\mathbf{q}})$$

$$\times \frac{n_F(sE_{\mathbf{k}}^\alpha) - n_F(-\xi_{\mathbf{q}-\mathbf{k}}^\gamma)}{q_0 - sE_{\mathbf{k}}^\alpha - \xi_{\mathbf{q}-\mathbf{k}}^\gamma}, \quad (2.36)$$

Furthermore, the gap equation (2.30) suggests that we can make the following Taylor expansion for $\chi(Q)$,

$$\chi(Q) = \chi(0) + Z \left(q_0 - \sum_{i=1}^3 \frac{1}{2m_{bi}} q_i^2 \right) + \dots, \quad (2.38)$$

where Z is a pair wave-function renormalization factor and m_{bi} is the effective ‘‘boson’’ mass parameter in the i direction. A straightforward calculation leads to

$$\chi(0) = \frac{-1}{2V} \sum_{\alpha,s=\pm} \sum_{\mathbf{k}} \frac{s}{2E_{\mathbf{k}}^\alpha} n_F(sE_{\mathbf{k}}^\alpha), \quad (2.39)$$

$$Z = \left. \frac{\partial \chi(Q)}{\partial q_0} \right|_{Q=0}$$

$$= \frac{1}{2V} \sum_{\alpha,s=\pm} \sum_{\mathbf{k}} \frac{s}{2E_{\mathbf{k}}^\alpha} \frac{n_F(E_{\mathbf{k}}^\alpha) - n_F(s\xi_{\mathbf{k}}^\alpha)}{E_{\mathbf{k}}^\alpha - s\xi_{\mathbf{k}}^\alpha} \quad (2.40)$$

$$\frac{Z}{2m_{bi}} = -\frac{1}{2} \left. \frac{\partial^2 \chi(Q)}{\partial q_i^2} \right|_{Q=0}$$

$$= -\frac{1}{8V} \sum_{\alpha,s=\pm} \sum_{\mathbf{k}} \left\{ \frac{s}{2E_{\mathbf{k}}^\alpha} \frac{\lambda_i^2}{\lambda^2 \mathbf{k}^2} \left(1 - \frac{\lambda_i^2 k_i^2}{\lambda^2 \mathbf{k}^2}\right) n_F(sE_{\mathbf{k}}^\alpha) - \frac{1}{2} \left(1 + s \frac{\xi_{\mathbf{k}}^\alpha}{E_{\mathbf{k}}^\alpha}\right) \frac{\lambda_i^2}{\lambda^2 \mathbf{k}^2} \left(1 - \frac{\lambda_i^2 k_i^2}{\lambda^2 \mathbf{k}^2}\right) \frac{n_F(sE_{\mathbf{k}}^\alpha) - n_F(-\xi_{\mathbf{k}}^\alpha)}{\xi_{\mathbf{k}}^\alpha + sE_{\mathbf{k}}^\alpha} \right.$$

$$- \frac{2s}{E_{\mathbf{k}}^\alpha} \left(\frac{k_i}{m} + \alpha \frac{\lambda_i^2 k_i}{\lambda |\mathbf{k}|} \right)^2 \left[\frac{n_F(sE_{\mathbf{k}}^\alpha) - n_F(-\xi_{\mathbf{k}}^\alpha)}{(sE_{\mathbf{k}}^\alpha + \xi_{\mathbf{k}}^\alpha)^2} + \frac{\beta n_F(\xi_{\mathbf{k}}^\alpha) n_F(-\xi_{\mathbf{k}}^\alpha)}{sE_{\mathbf{k}}^\alpha + \xi_{\mathbf{k}}^\alpha} \right]$$

$$\left. + \frac{s}{E_{\mathbf{k}}^\alpha} \left(\frac{1}{m} + \alpha \frac{\lambda_i^2}{\lambda |\mathbf{k}|} - \alpha \frac{\lambda_i^4 k_i^2}{\lambda^3 |\mathbf{k}|^3} \right) \frac{n_F(sE_{\mathbf{k}}^\alpha) - n_F(-\xi_{\mathbf{k}}^\alpha)}{sE_{\mathbf{k}}^\alpha + \xi_{\mathbf{k}}^\alpha} \right\}. \quad (2.41)$$

According to this Taylor expansion, we apply the pole approximation to the pair propagator or T matrix $t_{\text{pg}}(Q)$,

$$t_{\text{pg}}(Q) \simeq \frac{Z^{-1}}{q_0 - \sum_{i=1}^3 q_i^2 / (2m_{bi})}. \quad (2.42)$$

We stress here that in general, the small Q expansion of $t_{\text{pg}}^{-1}(Q)$ should contain a term $\propto q_0^2$. Without this term, Eq. (2.42) does not respect the particle-hole symmetry and thus can work, in principle, only when the system becomes bosonic. At the BCS limit, the system possesses a sharp Fermi

surface, the pair propagator should asymptotically recover the particle-hole symmetry, *i.e.*, the q_0^2 term should be kept. However, since at BCS limit the pseudogap is expected to be very small, applying Eq. (2.42) does not bring much quantitative difference. Therefore, we will apply Eq. (2.42) to the whole crossover region. We also note that the pole approximation to the pair propagator generally strengthens the uncondensed pairing and thus leads to amplification of the pseudogap effects, however, it remains a very good approximation for our qualitative and semi-quantitative analysis.

Substituting the number density equation, the parameter Z can be expressed as

$$Z = \frac{1}{\Delta^2} \left[\frac{n}{2} - \frac{1}{2V} \sum_{\alpha=\pm} \sum_{\mathbf{k}} n_F(\xi_{\mathbf{k}}^{\alpha}) \right]. \quad (2.43)$$

The expression in the square bracket of the right-hand side is nothing but the density of the pairs n_b , we thus have $n_b = Z\Delta^2$.

Substituting Eq. (2.42) into Eq. (2.32) leads to

$$\begin{aligned} \Delta_{\text{pg}}^2 &= \frac{1}{ZV} \sum_{\mathbf{q}} n_B \left[\sum_{i=1}^3 q_i^2 / (2m_{bi}) \right] \\ &= \frac{1}{Z} \prod_{i=1}^3 \sqrt{\frac{Tm_{bi}}{2\pi}} \zeta \left(\frac{3}{2} \right), \end{aligned} \quad (2.44)$$

where $n_B(x) = 1/[\exp(\beta x) - 1]$ is the Bose-Einstein function and a vacuum term was regularized out. It should be stressed that at zero temperature $\Delta_{\text{pg}}^2 = 0$, hence the G_0G scheme yields the BCS ground state. It is also worth noting that $\Delta_{\text{pg}}^2 = n_b^{\text{uncondensed}}/Z$, and hence $\Delta_{\text{sf}}^2 = n_b^{\text{condensed}}/Z$.

Now, Eq. (2.34), Eq. (2.35), as well as Eq. (2.44) are coupled to determine the total excitation gap Δ , the pseudogap Δ_{pg} and the chemical potential μ at a given temperature below T_c , and T_c itself is determined by the vanishing of Δ_{sf} .

C. G_0G formalism at $T \gtrsim T_c$

Above T_c , Eq. (2.30) does not apply, hence Eq. (2.31) no longer holds. To proceed, we extend our more precise $T \leq T_c$ equations to $T > T_c$ in a simplest fashion. We will continue to use Eq. (2.33) to parameterize the self-energy but with $\Delta = \Delta_{\text{pg}}$, and ignore the finite lifetime effect associated with normal state pairs. In the absence of the SOC, it was shown that this is a good approximation when temperature is not very much higher than T_c [24, 26]. The T matrix $t_{\text{pg}}(Q)$ at small Q can be approximated now as

$$t_{\text{pg}}(Q) \simeq \frac{Z^{-1}}{q_0 - \Omega_{\mathbf{q}}}, \quad (2.45)$$

where $\Omega_{\mathbf{q}} = \sum_{i=1}^3 q_i^2 / (2m_{bi}) - \mu_b$. Since there is no condensation in normal state, the effective pair chemical potential μ_b

is no longer zero, instead, it should be calculated from

$$\begin{aligned} Z\mu_b &\equiv t^{-1}(0) = \frac{1}{U} + \chi(0) \\ &= \frac{1}{U} - \frac{1}{2V} \sum_{\alpha, s=\pm} \sum_{\mathbf{k}} \frac{s}{2E_{\mathbf{k}}^{\alpha}} n_F(sE_{\mathbf{k}}^{\alpha}). \end{aligned} \quad (2.46)$$

This is used as the modified gap equation. Similarly, above T_c the pseudogap Δ_{pg} is determined by

$$\begin{aligned} \Delta_{\text{pg}}^2 &= \frac{1}{ZV} \sum_{\mathbf{q}} n_B(\Omega_{\mathbf{q}}) \\ &= \frac{1}{Z} \prod_{i=1}^3 \sqrt{\frac{Tm_{bi}}{2\pi}} \text{Li}_{\frac{3}{2}} \left(e^{\mu_b/T} \right), \end{aligned} \quad (2.47)$$

where $\text{Li}_n(z)$ is the polylogarithm function. Then Eq. (2.46), Eq. (2.47) and the number equation which remains unchanged determine Δ_{pg} , μ and μ_b at $T > T_c$.

At this point, we comment that at $T \gtrsim T_c$, the pseudogap may be closely related to the contact intensity \mathcal{C} which is introduced by Tan [45] through the large momentum tail of the distribution functions, $n_{\uparrow, \downarrow}(\mathbf{k}) \rightarrow \mathcal{C}/k^4$, $\mathbf{k} \rightarrow \infty$, and underlies a variety of universal thermodynamical relations for the Fermi gases. To see this, we recall the relation [46–48] that $\mathcal{C} = -(m^2/\beta V) \sum_Q \Gamma_{\text{pair}}(Q)$ with Γ_{pair} being the full propagator of the pairs. At $T \gtrsim T_c$, if we approximate Γ_{pair} by t_{pg} , we can roughly estimate the contact intensity as $\mathcal{C} \sim m^2 \Delta_{\text{pg}}^2$.

III. RESULTS AND DISCUSSIONS

With all the equations settled down, we now present the predictions obtained by solving them numerically. We will focus on three different types of SOC: EP ($\lambda_x = \lambda_y = 0, \lambda_z = \lambda$), EO ($\lambda_x = \lambda_y = \lambda, \lambda_z = 0$), and S ($\lambda_x = \lambda_y = \lambda_z = \lambda$). In all these cases, we regularize the UV divergence in the gap equations by introducing the s -wave scattering length a through

$$\frac{1}{U} = \frac{m}{4\pi a} - \frac{1}{V} \sum_{\mathbf{k}} \frac{m}{k^2}. \quad (3.1)$$

A. Analytical Results in the Molecular BEC limit

Let us first examine the molecular BEC limit which can be achieved by either tuning $1/(k_{\text{F}}a) \rightarrow +\infty$ for fixed SOC or tuning $\lambda \rightarrow \infty$ for fixed $1/(k_{\text{F}}a)$ for EO and S SOCs. The former case is well studied and here we are mainly interested in the latter case. In the molecular BEC limit, we expect $\mu < 0$ and $|\mu| \gg T_c$. For temperature around or below T_c , we can approximate $\xi_{\mathbf{k}}^{\alpha}/T, E_{\mathbf{k}}^{\alpha}/T \approx \infty$, and all the equations become temperature independent. In this limit, the gap equation determines the chemical potential while the number equation determines the gap. By further expanding the equations in powers of $\Delta/|\mu|$ and keeping several leading terms, we obtain some analytical results for various quantities at $T \lesssim T_c$.

(Some of them are already reported in Refs. [9–12, 17, 21].)
(I) S case. The chemical potential is well given by

$$\mu \approx -\frac{E_B}{2}, \quad (3.2)$$

where E_B is the binding energy determined by the two-body problem [9, 17, 21],

$$E_B = m\lambda^2 + \frac{1}{4m} \left(\frac{1}{a} + \sqrt{\frac{1}{a^2} + 4m^2\lambda^2} \right)^2. \quad (3.3)$$

The effective pair mass m_b coincides with the molecular effective mass determined at the two-body level. We have

$$\frac{2m}{m_b} \approx \frac{7}{3} - \frac{4}{3} \left(\frac{E_B - m\lambda^2}{E_B} \right)^{3/2} - \frac{2m\lambda^2}{E_B}. \quad (3.4)$$

Other quantities such as Δ and Z can be evaluated as

$$\Delta^2 \approx \frac{32\varepsilon_F \sqrt{\varepsilon_F}}{3\pi E_B} \left(\frac{E_B - m\lambda^2}{2} \right)^{3/2}, \quad (3.5)$$

$$Z \approx \frac{n}{2\Delta^2} = \frac{E_B}{8\pi} \left(\frac{m}{E_B - m\lambda^2} \right)^{3/2}. \quad (3.6)$$

(II) EO case. The chemical potential is also given by

$$\mu \approx -\frac{E_B}{2}, \quad (3.7)$$

where two-body binding energy E_B is determined by the algebra equation [9–11, 21],

$$\sqrt{\frac{E_B}{m\lambda^2}} - \frac{1}{2} \ln \frac{\sqrt{E_B} + \sqrt{m\lambda^2}}{\sqrt{E_B} - \sqrt{m\lambda^2}} = \frac{m}{\lambda a}. \quad (3.8)$$

The effective pair mass becomes anisotropic and is given by

$$m_b^\perp \approx 2m \left[1 - \frac{m\lambda^2}{2E_B} - \frac{E_B - m\lambda^2}{2E_B} \ln \frac{E_B - m\lambda^2}{E_B} \right]^{-1},$$

$$m_b^\parallel \approx 2m. \quad (3.9)$$

Other quantities such as Δ and Z can be evaluated as

$$\Delta^2 \approx \frac{8\varepsilon_F(E_B - m\lambda^2)}{3\pi} \sqrt{\frac{2\varepsilon_F}{E_B}}, \quad (3.10)$$

$$Z \approx \frac{n}{2\Delta^2} = \frac{\sqrt{m^3 E_B}}{8\pi(E_B - m\lambda^2)}. \quad (3.11)$$

(III) EP case. We find that the EP case is trivial. Increasing λ can not induce a BCS-BEC crossover. For large and positive $1/(k_F a)$, the EP SOC only induce a shift for the chemical potential,

$$\mu \approx -\frac{1}{2ma^2} - \frac{m\lambda^2}{2}. \quad (3.12)$$

The pair effective mass is almost isotropic and is given by

$$m_b^\perp \approx m_b^\parallel \approx 2m. \quad (3.13)$$

Other quantities such as Δ and Z just recover the usual results without SOC,

$$\Delta^2 \approx \frac{8\varepsilon_F k_F}{3\pi ma}, \quad (3.14)$$

$$Z \approx \frac{m^2 a}{8\pi}. \quad (3.15)$$

The critical temperature in the BEC limit, T_{BEC} , is determined by the number equation

$$n_B = \frac{1}{V} \sum_{\mathbf{k}} \frac{1}{\exp\left[\frac{\varepsilon_B(\mathbf{k})}{T_{\text{BEC}}}\right] - 1}, \quad (3.16)$$

where $\varepsilon_B(\mathbf{k}) = \sum_{i=1}^3 k_i^2 / (2m_{bi})$. This leads to $T_{\text{BEC}} = 2\pi[n_B / (\sqrt{\prod_i m_{bi}} \zeta(3/2))]^{3/2}$ in three dimensions. Setting $n_B = n/2$, we obtain

$$T_{\text{BEC}} \approx 0.218\varepsilon_F \prod_{i=1}^3 \left(\frac{2m}{m_{bi}} \right)^{1/3}. \quad (3.17)$$

Therefore, in the molecular BEC limit, T_{BEC} is only a function of the combined dimensionless parameter $\eta = 1/(m\lambda a)$. For S SOC we have

$$m_b = \begin{cases} 6m, & \eta \rightarrow -\infty \\ 2m, & \eta \rightarrow +\infty \\ 2.32m, & \eta \rightarrow 0 \end{cases} \quad (3.18)$$

and hence

$$T_{\text{BEC}} = \begin{cases} 0.0726\varepsilon_F, & \eta \rightarrow -\infty \\ 0.218\varepsilon_F, & \eta \rightarrow +\infty \\ 0.188\varepsilon_F, & \eta \rightarrow 0. \end{cases} \quad (3.19)$$

For EO SOC, we obtain

$$m_b^\perp = \begin{cases} 4m, & \eta \rightarrow -\infty \\ 2m, & \eta \rightarrow +\infty \\ 2.40m, & \eta \rightarrow 0 \end{cases} \quad (3.20)$$

and

$$T_{\text{BEC}} = \begin{cases} 0.137\varepsilon_F, & \eta \rightarrow -\infty \\ 0.218\varepsilon_F, & \eta \rightarrow +\infty \\ 0.193\varepsilon_F, & \eta \rightarrow 0. \end{cases} \quad (3.21)$$

As we will see, the above obtained T_{BEC} coincide well with our numerical results in Sec. III B.

B. Superfluid Critical Temperature

By numerically solving the set of coupled gap, number density, and pseudogap equations, we can obtain the superfluid order parameter Δ_{sf} , the pseudogap Δ_{pg} , and the fermion chemical potential μ . The superfluid critical temperature T_c is determined by the vanishing of the superfluid order parameter Δ_{sf} . The numerical results for T_c/ε_F as a function of the gas parameter $1/(k_F a)$ is shown in Fig. 2 for $\lambda = 0$ and $\lambda = v_F$.

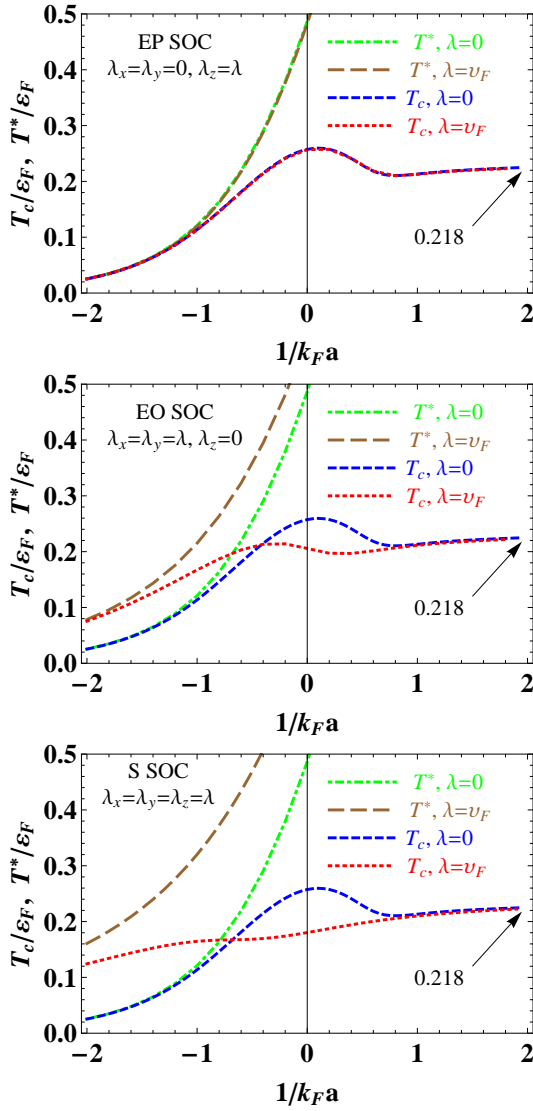


FIG. 2: (Color online) The critical temperature T_c scaled by the Fermi energy ε_F as a function of the gas parameter $1/(k_F a)$ for fixed SOC $\lambda = 0$ and $\lambda = v_F$. Also shown is the pair dissociation temperature T^* .

T_c/ε_F as a function of the SOC λ is shown in Fig. 3 for fixed $1/(k_F a) = -2$ and $1/(k_F a) = \infty$. Also shown is the critical temperature predicted by the BCS theory, T^*/ε_F , which is determined by the vanishing of Δ_{mf} . It is monotonously increasing as $1/(k_F a)$ or λ/v_F increased. The BCS theory loses the pairing-fluctuation effect and does not give reliable critical temperature particularly at large $1/(k_F a)$ or λ/v_F where T_c is mainly determined by the bosonic degrees of freedom.

For all three types of SOC, we find that T_c is a smooth function of $1/(k_F a)$ and λ/v_F , and the superfluid phase transition is always of second order for the whole crossover region (see next subsection). Also, it can be seen that T_c is not a monotonous function of $1/(k_F a)$ when λ is small: There is a local maximum in T_c curve around the unitary point. Simi-

lar local maximum also appears when one uses the Nozieres-Schmitt-Rink approach to determine T_c in the absence of SOC. It may be understood by noticing that the BEC critical temperature is increased when repulsive interactions between bosons are turned on [49]. We note that for a Rashba spin-orbit coupled Fermi gas, the superfluid transition temperature has been roughly estimated by approximating the system as a non-interacting mixture of fermions and rashbons and has been found to increase monotonously across the BCS-BEC crossover [11].

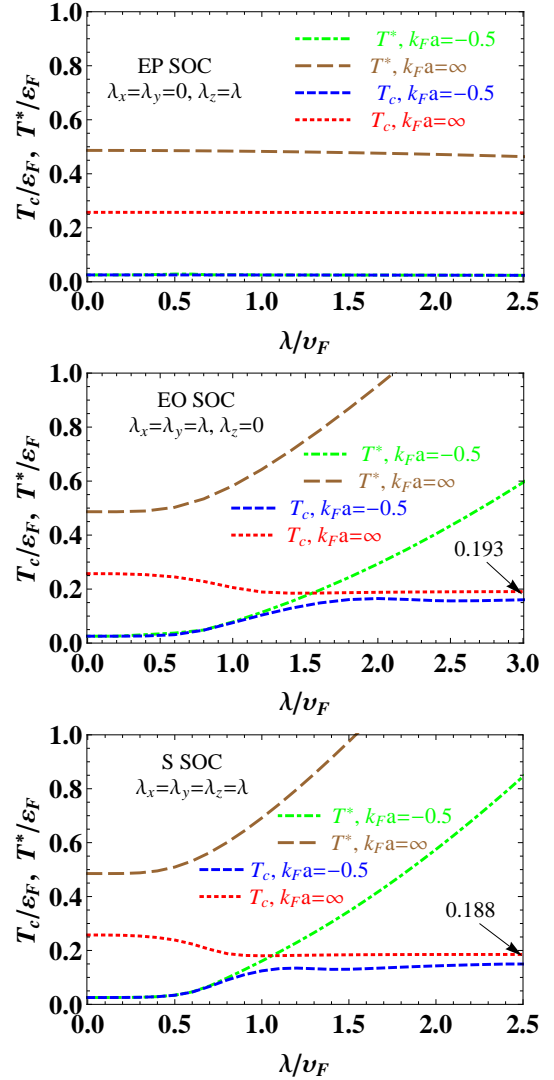


FIG. 3: (Color online) The critical temperature T_c and the dissociation temperature T^* scaled by the Fermi energy ε_F as a function of the SOC λ/v_F for fixed gas parameters $1/(k_F a) = -2$ and $1/(k_F a) = 0$.

From the top panels of Fig. 2 and Fig. 3 we see that the EP SOC does not affect T_c and T^* . This is consistent with the observation that EP SOC solely does not lead to new novel bound state and the fermion excitation gap does not change [21]. This can be understood by noticing that the EP

SOC in Hamiltonian (2.1) can be gauged away by using the gauge transformation $\psi_\uparrow \rightarrow e^{-im\lambda z}\psi_\uparrow$ and $\psi_\downarrow \rightarrow e^{im\lambda z}\psi_\downarrow$, resulting only a constant shift in the chemical potential, $\mu \rightarrow \mu + m\lambda^2/2$.

For the EO and S SOC, we observe from Fig. 2 that, comparing to the case without SOC, the SOC suppresses T_c for $k_F a$ close to unitarity while increases T_c at the BCS regime. To further understand how T_c is influenced by the SOC, we turn to Fig. 3. From Fig. 3 we see that T_c is not sensitive to λ for $\lambda \ll v_F$ and $\lambda \gg v_F$, but becomes sensitive to λ for $\lambda \sim v_F$: One can identify a BCS-BEC crossover solely induced by λ around $\lambda \approx v_F$. This coincides with previous zero-temperature studies [9–18]. Although at large negative $1/(k_F a)$, T_c increases (almost) monotonously as λ grows, near the resonance, we find that T_c is a decreasing function of λ , in contrast Ref. [50] where the authors predicted an increasing T_c along with λ . We note that for large enough λ , our result converges correctly to a universal molecular limit T_{BEC} either near the unitarity or at the BCS regime (see Sec. III A).

It should be stressed that T^* sets a lower bound for the pair dissociation temperature above which the pairs essentially dissociate due to thermal excitations. Previous study in the absence of the SOC shows that it is a good approximation to set T^* on the BCS side or near unitarity as the pair dissociation temperature [24, 26]. So we refer to T^* as the pair dissociation temperature in Fig. 2 and Fig. 3. The region between T_c and T^* is a pseudogap dominated window in which a normal state is no longer described by the Landau Fermi liquid theory. Fig. 2 and Fig. 3 show that even for large negative $1/(k_F a)$ the pseudogap dominated region can be sizable once the SOC is large. Thus, the spin-orbit coupled Fermi gas may provide a new platform to study the formation of pseudogap in fermionic systems.

C. Pseudogap

In this subsection, we focus on S and EO SOC because EP SOC does not bring qualitatively new features to the temperature dependence of the pseudogap than the $\lambda = 0$ case. In Fig. 4-Fig. 7, we plot Δ , Δ_{sf} , and Δ_{pg} as well as Δ_{BCS} (in units of ε_F , the same below) as functions of temperature.

The common feature for all these figures is that Δ_{sf} monotonically decrease to zero at T_c . Below T_c , $\Delta_{\text{pg}}(T)$ is a monotonically increasing function from zero at $T = 0$ where it vanishes according to $\Delta_{\text{pg}} \propto T^{3/4}$ (see Eq. (2.44)). Above T_c , $\Delta_{\text{pg}}(T)$ is a monotonically decreasing function from its maximum value located at T_c . This kind of temperature dependence clearly shows that pseudogap is due to the thermally excited pairs: Below T_c when T goes higher more pairs are excited from the condensate and at T_c all condensed pairs are thermally excited; after that the thermal motion of the pair participants begins to dissociate the pairs and hence Δ_{pg} (more precisely, $Z\Delta_{\text{pg}}^2$) begins to decrease. Although the physical pictures are clear, at temperature much higher than T_c our formalism may fail since the finite life-time of the pairs, which is not included in our formalism, may become important.

By comparing Fig. 5-Fig. 6 to Fig. 4 and by comparing two

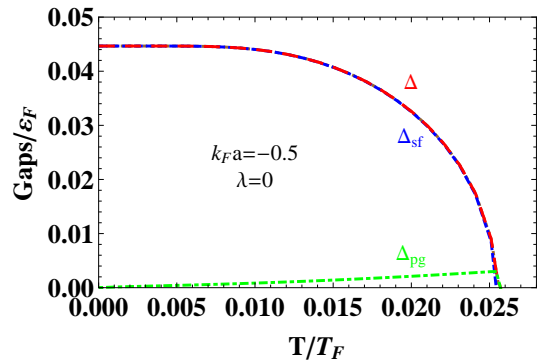


FIG. 4: (Color online) The temperature dependence of Δ , Δ_{sf} , and Δ_{pg} scaled by the Fermi energy for a Fermi gas without SOC at $k_F a = -0.5$.

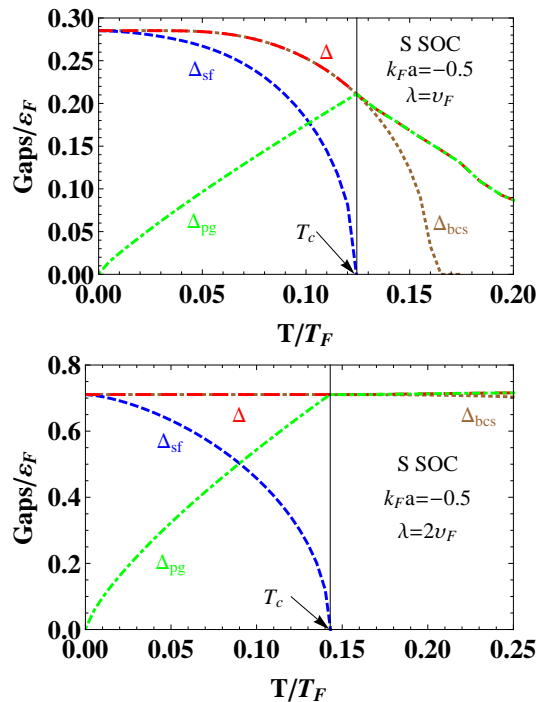


FIG. 5: (Color online) The temperature dependence of Δ , Δ_{sf} , and Δ_{pg} as well as Δ_{BCS} scaled by the Fermi energy at $k_F a = -0.5$ for S SOC.

bottom panels of Fig. 7 to the panel on the top, one can see that although the SOC does not modify the general tendency of the temperature dependence of the gaps, large SOC significantly enlarges the pseudogap window in the normal phase. Such pseudogap window may be detected by RF spectroscopy measurements, which we now turn to study.

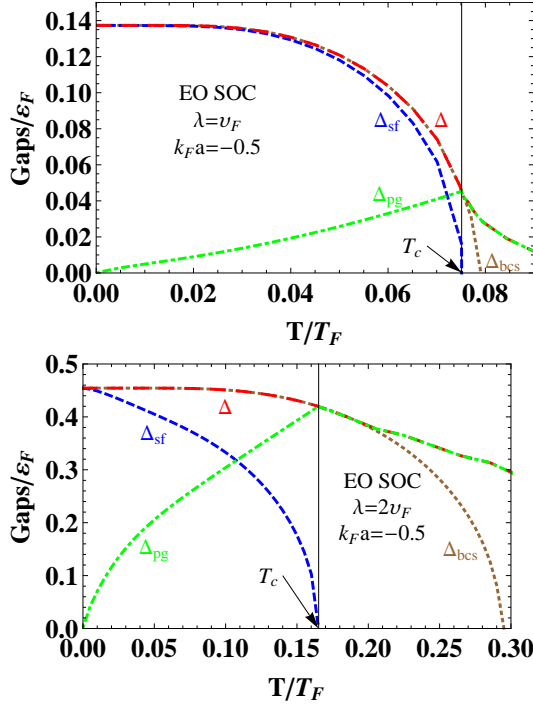


FIG. 6: (Color online) The temperature dependence of Δ , Δ_{sf} , Δ_{pg} , and Δ_{BCS} scaled by the Fermi energy at $k_F a = -0.5$ for EO SOC.

D. RF Spectroscopy

The radio-frequency (RF) spectroscopy has been proven to be very successful in probing the fermionic pairing, quasi-particle excitation spectrum, and superfluidity. For an atomic Fermi gas with two hyperfine states, $|\uparrow\rangle$ and $|\downarrow\rangle$, the RF laser drives transitions between one of the hyperfine states (i.e., $|\downarrow\rangle$) and an empty hyperfine state $|3\rangle$ which lies above it by an energy $\omega_{\downarrow 3}$ (which is set to zero because it can be absorbed into the chemical potential) due to the magnetic field splitting in bare atomic hyperfine levels. The Hamiltonian for RF-coupling may be written as,

$$H_{RF} = V_0 \int d^3 \mathbf{r} \left[\psi_3^\dagger(\mathbf{r}) \psi_\downarrow(\mathbf{r}) + \text{H.C.} \right] \quad (3.22)$$

where $\psi_3^\dagger(\mathbf{r})$ is the field operator which creates an atom at the position \mathbf{r} and V_0 is the strength of the RF drive and is related to a Rabi frequency ω_R by $V_0 = \omega_R/2$.

Let us now assume that there is no interaction between the third state and the spin-up or spin-down states, i.e., there is no final state effect. This approximation sounds valid for ^{40}K atoms, where the s -wave scattering length between the spin-down state and the third hyperfine state is small (i.e., ~ 200 Bohr radii) [51]. Within this approximation and taking into account that the third state is not occupied initially, the transfer strength (integrated RF spectrum) per spin-down atom can be written by ($V_0 = 1$),

$$\Gamma(\omega) = \frac{1}{V n_\downarrow} \sum_{\mathbf{k}} \mathcal{A}_{\downarrow\downarrow}(\mathbf{k}, \xi_{\mathbf{k}} - \omega) n_F(\xi_{\mathbf{k}} - \omega), \quad (3.23)$$

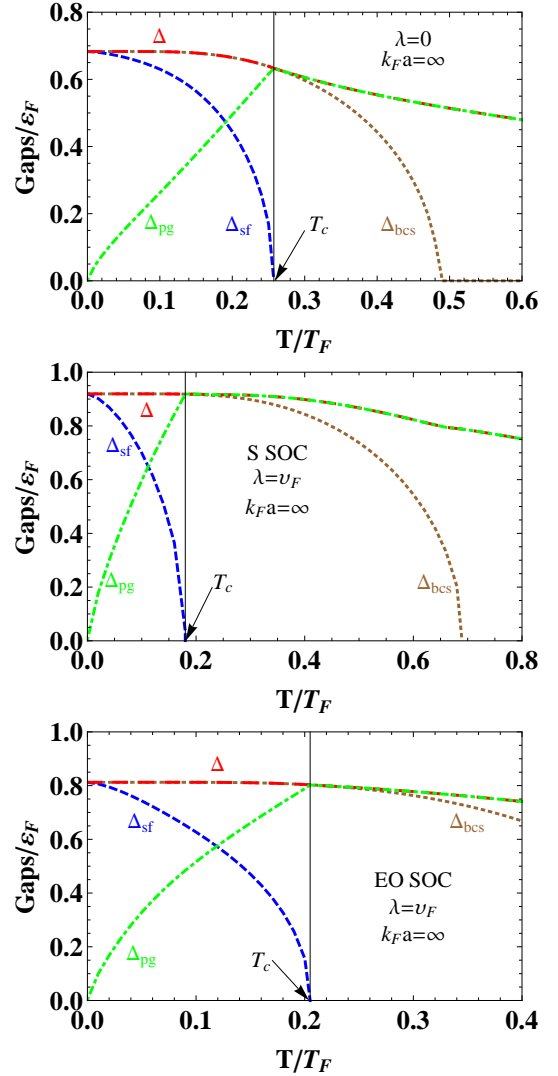


FIG. 7: (Color online) The temperature dependence of Δ , Δ_{sf} , Δ_{pg} , and Δ_{BCS} scaled by the Fermi energy at unitary point for $\lambda = 0$ Fermi gas and for EO- and S- SOC Fermi gases.

where n_\downarrow is the number density of the spin-down fermion and $\mathcal{A}_{\downarrow\downarrow} = -(1/\pi) \text{Im} \mathcal{G}_{\downarrow\downarrow}$ is the spectral function of the spin-down state². Note that

$$\int_{-\infty}^{\infty} d\omega \Gamma(\omega) = 1, \quad (3.24)$$

² Theoretical predictions for RF spectroscopy of single spin-orbit coupled bound fermion pair and of noninteracting spin-orbit coupled Fermi gas have been reported in Ref. [52]. Recently, the RF spectroscopy of equal Rashba and Dresselhaus spin-orbit coupled Fermi gases has been studied experimentally and theoretically in Ref. [53]. The theory part is based on a formalism similar with what we used here.

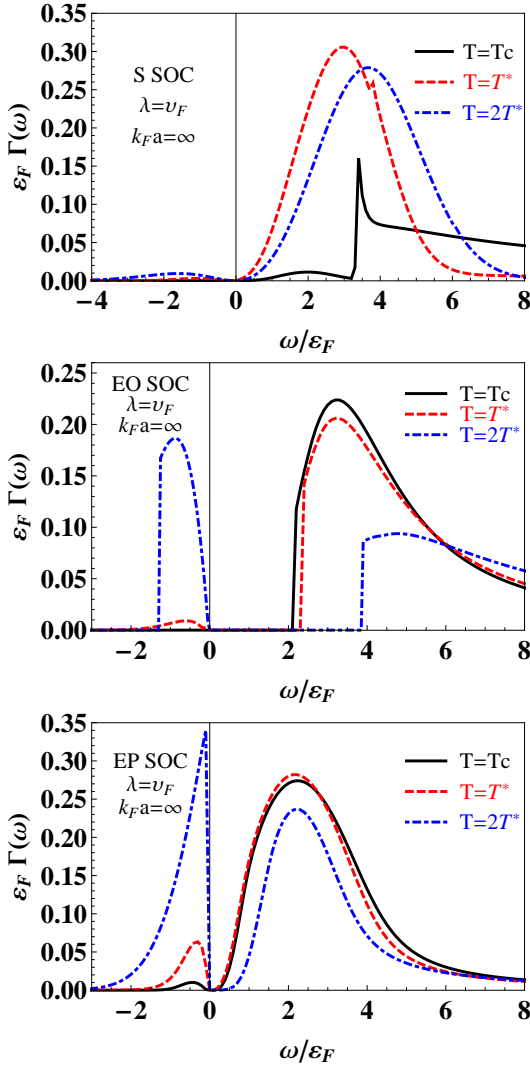


FIG. 8: (Color online) The RF spectrum $\Gamma(\omega)$ in unit of $1/\varepsilon_F$ for SO coupled unitary Fermi gases at resonance.

because

$$n_{\downarrow} = \frac{1}{V} \int_{-\infty}^{\infty} d\omega \sum_{\mathbf{k}} \mathcal{A}_{\downarrow\downarrow}(\mathbf{k}, \omega) n_F(\omega). \quad (3.25)$$

In Fig. 8, we present the integrated RF spectra for three different SOCs at resonance and at T_c , T^* , and $2T^*$. The RF spectra are calculated in an idealized manner (see Appendix A), *i.e.*, we neglect the final state interaction and width of the uncondensed pairs. Taking into account the effects of finite width may change the shape of the RF spectra, however, most of the qualitative features shall retain.

It is seen from Fig. 8 that the RF spectra consist of two continuum branches, one positive and another negative. The positive branches correspond to the “binding” fermion pairs contribution, while the negative branches can be regarded as the response of the thermal excited quasi-particles with a pseu-

dogap Δ_{pg} reflected in the positions of the negative branch peaks. With increasing temperature, more quasi-particles are excited, leading to a much more pronounced response appearing in the negative branches. Such a temperature-sensitive feature of the RF spectroscopy may provide a useful way to experimentally measure the critical temperature and to detect the existence of pseudogap in the normal phase.

IV. SUMMARY

We have theoretically investigated thermal effects on the BCS-BEC crossover of spin-orbit coupled Fermi gases. For this purpose, we have employed a T -matrix formalism based on a G_0G approximation for the pair susceptibility, which was thoroughly used in the previous studies of Fermi gases without SOC. This formalism extends the standard BCS theory by appropriately decomposing the excitation gap to a condensation part and a pseudogap part that characterize the pairing fluctuations.

Comparing to the BCS theory, our G_0G formalism predicts lower and more reliable critical temperature T_c for the superfluid-normal phase transition. The results for T_c have been presented in Fig. 2 to Fig. 3. At various molecular BEC limits, our predictions correctly recover the BEC temperature T_{BEC} of free Bose gases. The pseudogap persists not only in the superfluid phase ($T < T_c$) but also in a window of the normal phase ($T_c < T < T^*$) where it represents the existence of non-condensed, preformed pairs which dissociate above T^* . We have studied how the SOC influences the emergence of the pseudogap, as shown in Fig. 4-Fig. 7. It is seen that strong S- or EO- type SOC can significantly enlarge the pseudogap window in the normal phase. Thus, spin-orbit coupled Fermi gases provide a new platform to study the pseudogap physics. Experimentally, such pseudogap might be revealed by RF spectroscopy measurements. We have presented our qualitative predictions on the RF spectra in Fig. 8, which may be easily tested in future experiments.

Acknowledgments: LH and XGH are supported by the Helmholtz International Center for FAIR within the framework of the LOEWE program (Landesoffensive zur Entwicklung Wissenschaftlich- Ökonomischer Exzellenz) launched by the State of Hessen. XGH is also supported by Indiana University Grant No. 22-308-47 and the US DOE Grant No. DE-FG02-87ER40365. XJL and HH are supported by the ARC Discovery Projects DP0984637 and DP0984522.

Appendix A: Expressions for the RF spectroscopy

In this appendix, we list some expressions for the idealized RF spectroscopy for Fermi gases with and without SOC. Some of them are used in Sec.III D. By “idealized”, we mean that these expressions neglect the effects due to final state interactions and due to the finite lifetime effects of the uncondensed pairs.

(I) Without SOC. The spectral function of spin-down fermion is given by

$$\mathcal{A}_{\downarrow\downarrow}^0(\mathbf{k}, \omega) = u_{\mathbf{k}}^2 \delta(\omega - E_{\mathbf{k}}) + v_{\mathbf{k}}^2 \delta(\omega + E_{\mathbf{k}}). \quad (\text{A1})$$

The RF spectrum:

$$\Gamma_0(\omega) = \frac{m^{3/2}}{4\pi^2} \frac{\Delta^2}{\omega^2} \sqrt{\frac{\omega^2 - \Delta^2 + 2\mu\omega}{\omega}} n_F \left(-\frac{\omega^2 + \Delta^2}{2\omega} \right) \Theta \left(\frac{\omega^2 - \Delta^2 + 2\mu\omega}{\omega} \right). \quad (\text{A2})$$

(II) S SOC. The spectral function spin-down fermion is given by

$$\mathcal{A}_{\downarrow\downarrow}^S(\mathbf{k}, \omega) = \frac{1}{2} \sum_{\alpha} \left(1 - \alpha \frac{k_z}{|\mathbf{k}|} \right) [(u_{\mathbf{k}}^{\alpha})^2 \delta(\omega - E_{\mathbf{k}}^{\alpha}) + (v_{\mathbf{k}}^{\alpha})^2 \delta(\omega + E_{\mathbf{k}}^{\alpha})]. \quad (\text{A3})$$

The integrated RF spectrum:

$$\Gamma_S(\omega) = \frac{1}{4\pi^2 n_{\downarrow}} \sum_{\alpha} \int_0^{\infty} d|\mathbf{k}| |\mathbf{k}|^2 [(u_{\mathbf{k}}^{\alpha})^2 \delta(\xi_{\mathbf{k}} - \omega - E_{\mathbf{k}}^{\alpha}) + (v_{\mathbf{k}}^{\alpha})^2 \delta(\xi_{\mathbf{k}} - \omega + E_{\mathbf{k}}^{\alpha})] n_F(\xi_{\mathbf{k}} - \omega). \quad (\text{A4})$$

(III) EO SOC. The spectral function of spin-down fermion is given by

$$\mathcal{A}_{\downarrow\downarrow}^{\text{EO}}(\mathbf{k}, \omega) = \frac{1}{2} \sum_{\alpha} [(u_{\mathbf{k}}^{\alpha})^2 \delta(\omega - E_{\mathbf{k}}^{\alpha}) + (v_{\mathbf{k}}^{\alpha})^2 \delta(\omega + E_{\mathbf{k}}^{\alpha})]. \quad (\text{A5})$$

The integrated RF spectrum:

$$\begin{aligned} \Gamma_{\text{EO}}(\omega) &= \frac{\sqrt{2m}}{16\pi^2 n_{\downarrow}} \sum_{\alpha} \int_0^{\infty} dk_{\perp} k_{\perp} \frac{\Delta^2}{(\omega + \alpha \lambda k_{\perp})^2} n_F \left[-\frac{\Delta^2 + (\omega + \alpha \lambda k_{\perp})^2}{2(\omega + \alpha \lambda k_{\perp})} \right] \left[\frac{\omega^2 - \Delta^2 - \lambda^2 k_{\perp}^2}{2(\omega + \alpha \lambda k_{\perp})} - \frac{k_{\perp}^2}{2m} + \mu \right]^{-1/2} \\ &\times \Theta \left[\frac{\omega^2 - \Delta^2 - \lambda^2 k_{\perp}^2}{2(\omega + \alpha \lambda k_{\perp})} - \frac{k_{\perp}^2}{2m} + \mu \right]. \end{aligned} \quad (\text{A6})$$

(IV) EP SOC. The spectral function of spin-down fermion is given by:

$$\mathcal{A}_{\downarrow\downarrow}^{\text{EP}}(\mathbf{k}, \omega) = \frac{1}{2} \sum_{\alpha} \left(1 - \alpha \frac{k_z}{|\mathbf{k}|} \right) [(u_{\mathbf{k}}^{\alpha})^2 \delta(\omega - E_{\mathbf{k}}^{\alpha}) + (v_{\mathbf{k}}^{\alpha})^2 \delta(\omega + E_{\mathbf{k}}^{\alpha})]. \quad (\text{A7})$$

The integrated RF spectrum:

$$\Gamma_{\text{EP}}(\omega) = \frac{m^2}{8\pi^2 n_{\downarrow}} \sum_{\alpha} \int_0^{\infty} dk_z \frac{\Delta^2}{(\omega + \alpha \lambda k_z)^2} n_F \left[-\frac{\Delta^2 + (\omega + \alpha \lambda k_z)^2}{2(\omega + \alpha \lambda k_z)} \right] \Theta \left[\frac{\omega^2 - \Delta^2 - \lambda^2 k_z^2}{2(\omega + \alpha \lambda k_z)} - \frac{k_z^2}{2m} + \mu \right]. \quad (\text{A8})$$

-
- [1] D. M. Eagles, Phys. Rev. **186**, 456 (1969).
[2] A. J. Leggett, in *Modern trends in the theory of condensed matter*, Springer-Verlag, Berlin, 1980, pp.13-27.
[3] P. Nozieres and S. Schmitt-Rink, J. Low. Temp. Phys. **59**, 195 (1985).
[4] C. A. R. Sa de Melo, M. Randeria and J. R. Engelbrecht, Phys. Rev. Lett. **71**, 3202 (1993).
[5] M. Greiner, C. A. Regal and D. S. Jin, Nature **426**, 537 (2003).
[6] S. Jochim, M. Bartenstein, A. Altmeyer, G. Hendl, S. Riedl, C. Chin, J. Hecker Denschlag, and R. Grimm, Science **302**, 2101 (2003).
[7] M. W. Zwierlein, J. R. Abo-Shaeer, A. Schirotzek, C. H. Schunck, and W. Ketterle, Nature **435**, 1047 (2005).
[8] Y.-J. Lin, K. Jimenez-Garcia, and I. B. Spielman, Nature **471**, 83 (2011).
[9] J. P. Vyasanakere, S. Zhang, and V. B. Shenoy, Phys. Rev. **B84**, 014512 (2011); J. P. Vyasanakere and V. B. Shenoy, Phys. Rev. **A86**, 053617 (2012).

- [10] H. Hu, L. Jiang, X.-J. Liu, and H. Pu, Phys. Rev. Lett. **107**, 195304 (2011); L. Jiang, X. -J. Liu, H. Hu and H. Pu, Phys. Rev. A **84**, 063618 (2011); X. -J. Liu, L. Jiang, H. Pu, and H. Hu, Phys. Rev. A **85**, 021603(R) (2012); J.-X. Cui, X.-J. Liu, G. L. Long, and H. Hu, Phys. Rev. A **86**, 053628 (2012).
- [11] Z.-Q. Yu and H. Zhai, Phys. Rev. Lett. **107**, 195305 (2011).
- [12] M. Iskin and A. L. Subasi, Phys. Rev. Lett. **107**, 050402 (2011); Phys. Rev. **A84**, 041610(R) (2011); Phys. Rev. **A84**, 043621(2011); M. Iskin, Phys. Rev. **A86**, 065601 (2012).
- [13] M. Gong, S. Tewari, and C. Zhang, Phys. Rev. Lett. **107**, 195303 (2011); G. Chen, M. Gong, and C. Zhang, Phys. Rev. **A85**, 013601 (2012); M. Gong, G. Chen, S. Jia, and C. Zhang, Phys. Rev. Lett. **109**, 105302 (2012).
- [14] L. Han and C. A. R. Sa de Melo, Phys. Rev. **A85**, 011606(R)(2012); arXiv: 1206.4984; K. Seo, L. Han, and C. A. R. Sa de Melo, Phys. Rev. Lett. **109**, 105303 (2012).
- [15] W. Yi and G. -C. Guo, Phys. Rev. **A84**, 031608(R) (2011); J. Zhou, W. Zhang, and W. Yi, Phys. Rev. **A84**, 063603 (2011).
- [16] L. He and X. -G. Huang, Phys. Rev. Lett. **108**, 145302 (2012).
- [17] L. He and X. -G. Huang, Phys. Rev. B **86**, 014511 (2012); Phys. Rev. A **86**, 043618 (2012); arXiv:1207.2810.
- [18] L. Dell'Anna, G. Mazzarella, and L. Salasnich, Phys. Rev. **A84**, 033633 (2011); K. Zhou and Z. Zhang, Phys. Rev. Lett. **108**, 025301 (2012); B. Huang and S. Wan, arXiv: 1109.3970; X. Yang and S. Wan, Phys. Rev. **A85**, 023633 (2012).
- [19] P. Wang, Z.-Q. Yu, Z. Fu, J. Miao, L. Huang, S. Chai, H. Zhai, and J. Zhang, Phys. Rev. Lett. **109**, 095301 (2012).
- [20] L. W. Cheuk, A. T. Sommer, Z. Hadzibabic, T. Yefsah, W. S. Bakr, and M. W. Zwierlein, Phys. Rev. Lett. **109**, 095302 (2012).
- [21] J. P. Vyasankere and V. B. Shenoy, Phys. Rev. **B83**, 094515 (2011).
- [22] V. M. Loktev, R. M. Quick and S. G. Sharapov, Phys. Rept. **349**, 1 (2001).
- [23] I. Kosztin, Q. Chen, B. Janko and K. Levin, Phys. Rev. **B58**, 5936(R) (1998).
- [24] J. Maly, B. Janko and K. Levin, Physica **C321**, 113 (1999).
- [25] I. Kosztin, Q. Chen, Y. J. Kao and K. Levin, Phys. Rev. **B61**, 11662 (2000).
- [26] Q. J. Chen, J. Stajic, S. N. Tan and K. Levin, Phys. Rept. **412**, 1 (2005).
- [27] K. Levin, Q. Chen, Ch.Ch. Chien and Y. He, Ann. Phys. **325**, 233 (2010).
- [28] Ch. Ch. Chien, H. Guo, Y. He and K. Levin, Phys. Rev. **A81**, 023622 (2010).
- [29] H. Hu, X.-J. Liu, P. D. Drummond, and H. Dong, Phys. Rev. Lett. **104**, 240407(2010).
- [30] A. Perali, P. Pieri, G. C. Strinati, and C. Castellani, Phys. Rev. **B66**, 024510 (2002).
- [31] P. Magierski, G. Wlazlowski, A. Bulgac, and J. E. Drut, Phys. Rev. Lett. **103**, 210403(2009).
- [32] M. Feld, B. Fröhlich, E. Vogt, M. Koschorreck, and M. Köhl, Nature **480**, 75 (2011).
- [33] J. P. Gaebler, J. T. Stewart, T. E. Drake, D. S. Jin, A. Perali, P. Pieri, and G. C. Strinati, Nature Phys. **6**, 569 (2010); A. Perali, F. Palestini, P. Pieri, G. C. Strinati, J. T. Stewart, J. P. Gaebler, T. E. Drake, and D. S. Jin, Phys. Rev. Lett. **106**, 060402 (2011).
- [34] Q. Chen, I. Kosztin, B. Janko and K. Levin, Phys. Rev. Lett. **81**, 4708 (1998).
- [35] V. J. Emery and S. A. Kivelson, Nature **374**, 434 (1995); P. A. Lee, N. Nagaosa, T. K. Ng and X.-G. Wen, Phys. Rev. **B57**, 6003 (1998); S. Chakravarty, R. B. Laughlin, D. K. Morr and C. Nayak, Phys. Rev. **B63**, 094503 (2001).
- [36] A. Damascelli, Z. Hussain, and Z. -X. Shen, Rev. Mod. Phys. **75**, 473 (2003).
- [37] A. Schnell, G. Roepke, P. Schuck, Phys. Rev. Lett. **83**, 1926 (1999); X. -G. Huang, Phys. Rev. **C81**, 034007 (2010).
- [38] M. Kitazawa, T. Koide, T. Kunihiro, and Y. Nemoto, Phys. Rev. **D65**, 091504 (2002); *ibid* **70**, 056003 (2004); Prog. Theor. Phys. **114**, 117 (2005); L. He and P. Zhuang, Phys. Rev. **D76**, 056003 (2007).
- [39] L. P. Kadanoff and P. C. Martin, Phys. Rev. **124**, 670 (1961).
- [40] B. R. Patton, Phys. Rev. Lett. **27**, 1273 (1971).
- [41] J. P. Gaebler, Ph.D. thesis, University of Colorado, 2010.
- [42] F. Werner, L. Tarruell, and Y. Castin, Eur. Phys. J. **B68**, 401 (2009).
- [43] D. J. Thouless, Ann. Phys. (NY) **10**, 553 (1960).
- [44] J. Carlson, S.-Y. Chang, V. R. Pandharipande, and K. E. Schmidt, Phys. Rev. Lett. **91**, 050401 (2003).
- [45] S. Tan, Ann. Phys. (NY) **323**, 2952 (2008); **323**, 2971 (2008).
- [46] P. Pieri, A. Perali, and G. C. Strinati, Nat. Phys. **5**, 736 (2009).
- [47] R. Haussmann, M. Punk, and W. Zwerger, Phys. Rev. **A80**, 063612 (2009).
- [48] H. Hu, X.-J. Liu, and P. D. Drummond, New J. Phys. **13**, 035007 (2011).
- [49] J. O. Andersen, Rev. Mod. Phys. **76**, 599 (2004).
- [50] R. Liao, Y. Yi-Xiang, and W. -M. Liu, Phys. Rev. Lett. **108**, 080406 (2012).
- [51] I. Bloch, J. Dalibard, and W. Zwerger, Rev. Mod. Phys. **80**, 885 (2008).
- [52] X. -J. Liu, Phys. Rev. **A86**, 033613 (2012); H. Hu, H. Pu, J. Zhang, S. -G. Peng, and X. -J. Liu, Phys. Rev. **A86**, 053627 (2012); S. -G. Peng, X. -J. Liu, H. Hu, and K. Jiang Phys. Rev. **A86**, 063610 (2012).
- [53] Z. Fu, L. Huang, Z. Meng, P. Wang, X.-J. Liu, H. Pu, H. Hu, and J. Zhang, arXiv:1303.2212.